2016. Proceedings of the Indiana Academy of Science 125(1):1–18

MONITORING *IN VITRO* RESPONSE OF SELENIUM-TREATED HUMAN PROSTATE CELLS BY ^{1}H NMR SPECTROSCOPY

Meden F. Isaac-Lam[1] and **Patricia J. Green**[2]: Department of Chemistry and Physics, Purdue University Northwest, Westville, IN 46391 USA

Jonathan R. D. Kuhn: Department of Mathematics, Statistics and Computer Science, Purdue University Northwest, Westville, IN 46391 USA

John S. Harwood: Department of Chemistry and Purdue Interdepartmental NMR Facility, Purdue University, West Lafayette, IN 47907 USA

ABSTRACT. NMR metabolomics provides a potent method for monitoring alterations in the metabolic signature within tissues and biofluids. In this study, NMR analysis was utilized to determine variation in metabolite levels of human DU145 prostate cancer and non-tumorigenic PNT1A prostate epithelial cells after treatment with selenomethionine (SeM) and Se-methylselenocysteine (SeMSC). Currently, these are the first ^{1}H NMR spectroscopic data on selenium-treated prostate cell lines. Fluorescence microscopy of SeM-incubated PNT1A cells revealed morphological features characteristic of apoptosis. SeMSC-treated PNT1A and DU145 prostate cells indicated greater changes in cellular morphology and in metabolite levels than SeM-treated cells. NMR of prostate cells treated with selenium showed a decreasing trend in metabolite levels with the largest change exhibited by creatine. This is mainly due to disrupted energy metabolism, and probably due to loss of structural integrity combined with dissipation of metabolites. Lactate, choline-containing compounds, and glycine levels increased depending on the type of selenium and cell line used. No clear pattern of variation in metabolite concentration levels from ^{1}H NMR spectroscopy to distinguish apoptotic versus non-apoptotic pathway was observed. Factor analysis (FA) indicated the change in the concentration levels of twelve metabolites was able to distinguish DU145 cells from PNT1A cells when treated using SeM. This study indicated that NMR of intact cells treated with selenium can provide information on the biochemical processes of tissues; thus metabolic fingerprints for compromised cells can be acquired.

Keywords: NMR spectroscopy, metabolomics, selenomethionine, Se-methylselenocysteine, prostate cancer, apoptosis

INTRODUCTION

Selenium is an essential nonmetallic trace element necessary for normal metabolic functions in humans and animals. It serves as a cofactor for the antioxidant enzymes glutathione peroxidase and thioredoxin reductase. Its role in cancer prevention and treatment has gained attention in recent years based on cell culture and animal studies, epidemiological evidence, and human intervention findings demonstrating the anticarcinogenic potential of selenium (Rayman 2005; Jackson & Combs 2008; Zeng 2009; Sanmartin et al. 2012; Chen et al. 2013). The effectiveness of selenium as an anticancer agent has been refuted due to dismal findings from Selenium and Vitamin E Cancer Prevention Trial (SELECT), a phase III randomized placebo-controlled human trial investigating the chemopreventive effects of selenium, vitamin E, or combination of these dietary supplements against prostate cancer. However, post-SELECT studies suggested that the primary reason for its failure was the inadequate dose or formulation of selenium administered to produce optimum effect (Dunn et al. 2010; Ledesma et al. 2011; Hurst et al. 2012; Kristal et al. 2014). A recent report on a series of observational studies conducted on more than 1,100,000 volunteers showed lower cancer incidence and cancer mortality associated with higher selenium exposure (Vinceti et al. 2015). In addition, conflicting results including inverse, null, and direct associations have been reported for certain types of cancer. Therefore, the collection of more preclinical data on selenium is necessary for the scientific community to better understand its mechanism of action. Additional-

[1] *Corresponding author*: Meden F. Isaac-Lam, 219-785-5776 (phone), 219-785-5483 (FAX), isaaclam@pnw.edu.
[2] Undergraduate Student.

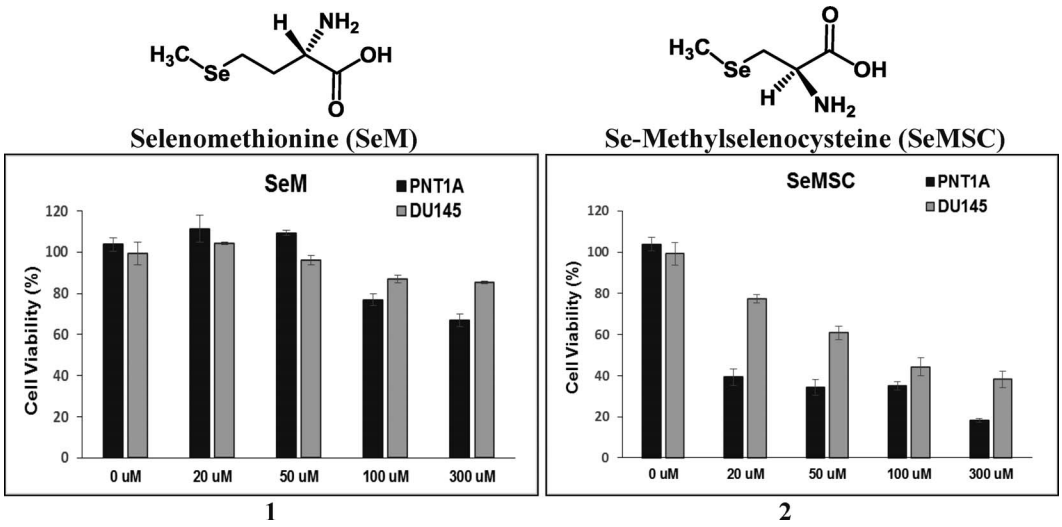

Figures 1–2.—Bar plots of cell survival assay of non-tumorigenic PNT1A and tumorigenic DU145 prostate cells upon incubation with 20-300 μM solutions of SeM (1) and SeMSC (2). The data represent the average corrected absorbance of eight wells carried out in triplicate independent experiments (96 wells/experiment) and based on untreated cells as controls; *bars*: ±SE.

ly, numerous existing investigations supporting the anti-proliferative effects of selenium against prostate cancer sufficiently justify further studies in this direction (Menter et al. 2000; Wang et al. 2002; Zhong & Oberley 2002; Meuillet et al. 2004; Reagan-Shaw et al. 2008; Richie et al. 2014; Singh et al. 2014), especially since prostate cancer (PCa) is the second leading cause of cancer deaths in US men as of 2011 (Siegel et al. 2015).

Selenomethionine (SeM) or Se-methylselenocysteine (SeMSC), two naturally prevalent organoselenium amino acids (Fig. 1) shown to have potential anticancer activity, are utilized in most experimental as well as clinical studies. SeM was the major component in dietary Se-supplementation in the completed SELECT trial in which participants were randomized to receive either 200 μg or 800 μg of selenized yeast or matched placebo per day. SeMSC is a naturally-occurring amino acid found in Brazil nuts, garlic, onion, and broccoli. Nutritional levels of selenium supplementation provide antioxidant protection against reactive oxygen damage, while supra-nutritional levels of 200 μg/day, about fourfold more than the recommended daily allowance (RDA), may initiate anticancer activity (Seo et al. 2002; Reid et al. 2004). According to the National Institutes of Health (NIH) dietary supplement fact sheet, the RDA of selenium for adults is 55–70 μg/day (NIH 2015). Previous experimental findings reported that SeM activates p53 tumor suppression protein (Seo et al. 2002), stimulates DNA repair response in human fibroblasts *in vitro* (Seo et al. 2002), induces cell-cycle arrest in human colon cancer cells (Goulet et al. 2005; Nelson et al. 2005), and apoptosis in lung (Yamamoto et al. 2003) and prostate cancer cells (Zhao et al. 2006). SeMSC, on the other hand, affects tumor growth by targeting androgen receptor signaling in prostate cancer cells (Lee et al. 2006), and stimulates apoptosis through caspase activation in human promyelocytic leukemia HL-60 cells (Kim et al. 2001) and in SKOV-3 ovarian cancer cells (Yeo et al. 2002). Different forms of selenium compounds were demonstrated to target different mechanisms to inhibit cell growth and proliferation of human DU145, PC-3, and LNCaP prostate cancer cell lines (Pinto et al. 2007; Li et al. 2008; Abdulah et al. 2011). However, investigations of the metabolomic profile response of prostate cancer cells as a result of selenium treatment are not yet available.

Metabolomics (Beger 2013; Vermeersch & Styczynski 2013), which involves simultaneous measurement of all the possible metabolites produced by living cells or tissues, has been successfully applied to prostate cancer research by utilizing nuclear magnetic resonance (NMR) spectroscopy (Jordan & Cheng 2007; Roberts et al. 2014; Lin & Chung 2014;). NMR analysis,

which is a non-invasive technique to study biological systems undergoing physiological transformation and involves inexpensive minimal sample preparation, has been widely used as a metabolic profiling tool to generate quantitative data of low-molecular weight metabolites produced by living cells (Palmnas & Vogel 2013; Shao et al. 2014). To date, the literature abounds with numerous NMR-based platforms to study PCa cells *in vitro* (Cornel et al. 1995; Ackerstaff et al. 2001; Milkevitch et al. 2005; Podo et al. 2011; Teahan et al. 2011; MacKinnon et al. 2012), *ex vivo* (Serkova et al. 2008; Levin et al. 2009; DeFeo & Chen 2010; DeFeo et al. 2011; Stenman et al. 2010, 2011; Giskeødegård et al. 2013), and *in vivo* (Zakian et al. 2008; Thomas et al. 2013). In spite of this, NMR-based metabolomic investigation into the alterations of the metabolic profile of PCa cells after selenium treatment has not been explored.

The objectives of this study were to monitor changes in metabolite levels upon selenium treatment of human DU145 prostate cancer cells and to compare with a non-tumorigenic PNT1A prostate cell line. Two organoselenium compounds, selenomethionine (SeM) and Se-methylselenocysteine (SeMSC), known to have anticancer properties (Zeng 2009; Sanmartin et al. 2012), were used for treatment. NMR spectroscopy detected reduced metabolite concentrations dependent upon the organoselenium used and the cell type. However, no clear pattern of metabolite change distinguished apoptotic versus non-apoptotic pathways.

METHODS

Cell line cultivation and sub-culturing.—Androgen-insensitive human prostate adenocarcinoma DU145 was purchased from the American Type Culture Collection (ATCC HTB-81). Normal PNT1A prostate epithelial cell line was obtained from Sigma (Cat No. 95012614). DU145 cells were cultured in EMEM (ATCC), while PNT1A cells were grown in RPMI 1640 medium (MediaTech, Inc.). Both media were supplemented with 10% fetal bovine serum (FBS, MediaTech, Inc.) and with 1% solution containing 10,000 IU/mL penicillin and 10,000 μg/mL streptomycin (MediaTech, Inc.). Cells were grown to 80–90% confluence ($\sim 2 \times 10^7$ cells) in 75-cm^2 culture flasks (Corning) for about a week (6–7 days) in a humidified incubator (Fisher Scientific Isotemp) with 5% CO_2 at 37° C. During the incubation period, growth media was changed once with fresh pre-warmed medium (pH 7.2). To harvest the cells, old growth media was aspirated and 5 mL 0.25% trypsin solution (Thermo Sci Hyclone) were added. The cells were incubated for an additional 10 min or until they visibly detached from the flask walls. Clumped cells were broken up gently and 1 mL of the trypsinized cell homogenate suspension was transferred into a new T75 cell culture flask containing pre-warmed media (20 mL) for further culturing.

Cell survival assay.—Cells were grown to confluence in a 96-well plate (2×10^3 cells/well) and incubated for 24 hrs with SeM or SeMSC (20, 50, 100 and 300 μM) in growth media from a stock solution of 10 mM in PBS (phosphate buffered saline, Fisher). Incubation period of 24 hrs for SeM and SeMSC was based on previous studies conducted by others to stimulate apoptosis using selenium compounds (Kim et al. 2001; Wang et al. 2002). The following day, cells were washed with pre-warmed PBS. MTT (3-[4,5-dimethyl-thiazol-2-yl]-2.5-diphenyltetrazolium bromide, Sigma, 0.5 mg/mL) in PBS was added to each well. Samples were allowed to incubate for an additional 2 hrs, after which dark blue crystals formed. DMSO was added to each well and allowed to stand at room temperature for 1 hr to dissolve the purplish-blue formazan crystals. Plates were shaken for 2 min and thereafter the absorbance values at 490 nm were measured on a microplate reader (BioRad 550). Absorbance readings were calculated based on the absorbance of the cells alone (as control) and were directly proportional to the number of viable cells in culture. Results were reported as average of triplicate measurements.

Fluorescence microscopy.—Cells (1 mL aliquots) obtained from a diluted cell suspension were seeded into each well (1.7 cm^2, ~1000 cells/well) of a 4-well culture slide (BD Biosciences) and grown to confluence in 5% CO_2 at 37° C for 6–7 days for attachment to the substratum. After aspirating the old growth media, 1 mL of SeM or SeMSC (20, 50, 100 and 300 μM) in fresh pre-warmed media at 37° C was added to each well. After incubation for 24 hrs, cells were washed twice with 1 mL fresh growth media. Cells were stained either with Hoechst 33258 (Molecular Probes) or trimethylrhodamine methylester perchlorate (TMRM, Setareh Biotech) or crystal violet (CV, Fisher). Cells were stained in the dark

with 1 mL of 0.1 mg/mL Hoechst 33258 or with 2 μM TMRM in pre-warmed media for 10 min at 37° C, washed twice with 1 mL filtered PBS, then fixed with 1 mL filtered pre-warmed 4% paraformaldehyde for 15 min in the incubator. For CV staining, cells were fixed first with methanol (5 min), and then stained with 0.05% crystal violet dissolved in methanol for 30 min after aspirating out methanol. After thorough liquid aspiration, the wells were removed and allowed to air dry in the dark for 1 hr. Slides were protected with coverslips, whose edges were sealed using a clear fast-drying nail polish and allowed to dry at room temperature in the dark for 30 min. Images were recorded by means of fluorescence microscopy (DAPI for Hoechst 350–390 nm excitation and 460–490 nm emission filters; Texas Red for TMRM 550–560 nm excitation and a 570–650 nm emission filters; and, phase contrast for CV) using an upright fluorescence microscope with Retiga imaging 2000R (Nikon Optiphot-2, 20× and 40×) and an image processing Nikon NIS-Elements V4.0 Qimaging software.

Treatment and preparation of cells for NMR spectroscopy.—Cells were grown to 80% confluence in Petri dishes (50 mm in diameter) in 4.5% CO_2 at 37° C for 5–6 days for full attachment to the substratum. After aspirating the old growth media, 3 mL of SeM or SeMSC (300 μM) in fresh pre-warmed media at 37° C was added to each dish. After incubation for 24 hrs, cells were washed twice with 0.5 mL PBS in D_2O (Cambridge Isotope Laboratories). D_2O (0.7 mL) was again added to each petri dish and cells were gently scraped from the surface with a sterile cell scraper. A volume of 0.7 mL of the harvested cell suspension was transferred into a 5 mm NMR tube and 10 μL of 100 mM TMSP in D_2O was added to each tube. Prior to NMR analysis, tubes were vortexed to ensure samples were in suspension. Control experiments using untreated cells were conducted in parallel with treated cells with the same incubation protocols and sample preparation. The protocol followed for the *in vitro* NMR analysis in this study was based on published procedure (Bezabeh et al. 2001; Al-Saffar et al. 2002; Rainaldi et al. 2008; Opstad et al. 2009) in which cells (control and treated) were analyzed on intact cell samples and not on an extract (i.e., perchloric acid extract), thereby eliminating alteration of metabolite levels caused by extraction (Whitehead & Kieber-Emmons 2005).

^{1}H NMR spectroscopy.—^{1}H NMR spectra were obtained on a Bruker AV-III-800 NMR spectrometer operating at 800.1337665 MHz and equipped with 5-mm TX1 probe. Gradient shimming was utilized prior to spectral acquisition. Chemical shifts (δ) are given in ppm relative to TMSP: $(CH_3)_3Si(CD_2)_2CO_2Na$, sodium 3-trimethylsilyl-propionate-2,2,3,3-d_4, set at 0 ppm. One-dimensional, one pulse ^{1}H NMR spectra were acquired using the zg one-pulse sequence available in the Bruker pulse sequence library. FIDs for the 1D spectra were collected at 298K by employing a relaxation delay of 2.0 s, a spectral width of 11160 Hz, a data size of 32 K, a pulse width of 90° (8.5 μs), and 256 scans. The FIDs were apodized with an exponential multiplication function using a line-broadening factor of 1.0 Hz prior to Fourier transformation. Water suppression for ^{1}H was carried out using the zgpr pulse sequence from the Bruker pulse sequence library.

Spectral analysis.—Each NMR sample consisted of approximately 10^6 cells and concentration of the metabolites was calculated using the formula:

$$[\text{Metabolite}] = (PA_M/PA_{TMSP}) \times (\text{Number of H's})_M / (\text{Number of H's})_{TMSP} \times [\text{TMSP}]$$

where [Metabolite] and [TMSP] are metabolite concentrations in mM of a metabolite and reference, respectively; and, PA refers to peak integration from NMR signal of the particular metabolite M or TMSP. Percent relative change after selenium treatment compared to untreated control cells was calculated by: % Relative Change = $(PA_{treated}\text{-}PA_{untreated}/PA_{untreated}) \times 100$.

Statistical analysis.—Library psych (1.4.3 library in R, W. Revelle (revelle@northwestern.edu, accessed March 2014) in statistical package R, version 3.0.3 (http://www.r-project.org/, accessed March 2014), with integrated development environment RStudio, version 0.98.932 (http://www.rstudio.com/, accessed March 2014), was used to perform factor analyses (FAs) of the average percent change of 12 metabolites in both normal epithelial PNT1A and prostate

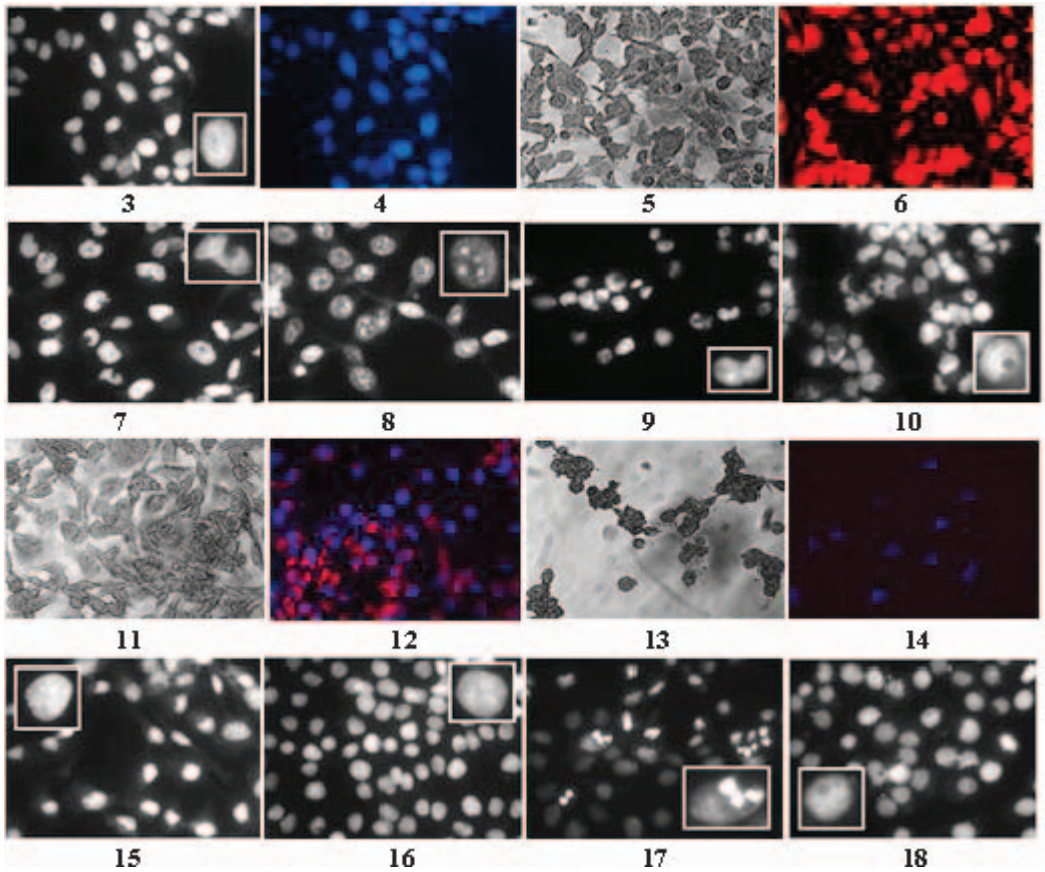

Figures 3–18.—Fluorescence microscopy images of fixed human prostate cells. Grayscale and blue fluorescence images of non-tumorigenic PNT1A cells alone stained with Hoechst (3 and 4, respectively), crystal violet (5), and TMRM (6). Cell morphology after 24 h incubation with SeM at 100 and 300 μM concentrations (7 and 8, respectively), and SeMSC at 100 and 300 μM concentrations (9 and 10, respectively). CV staining of cells with 300 μM SEM- and SeMSC-treated cells (11 and 13, respectively). TMRM/Hoechst double staining after treatment with 300 μM SeM (12) and SeMSC (14). DU145 PCa cells alone (15) and after 24 h incubation with SeM at 100 μM (16) and 300 μM (17), and with SeMSC at 300 μM (18) concentrations. Apoptotic cells are evident in 300 μM SeM-treated cells (8 & 17). Inserts indicate enlarged view of a single cell.

DU145 cancer cells incubated with SeM and SeMSC, replicated three times: PNT1A SeM trials 1, 2, and 3; PNT1A SeMSC trials 1, 2, and 3; DU145 SeM trials 1, 2, and 3; and, DU145 SeMSC trials 1, 2, and 3 (Kabacoff 2011).

RESULTS

Cell survival and morphology.—Cells were incubated with SeM and SeMSC at concentrations of 20–300 μM for 24 hrs. Cell survival assay (Figs. 1 & 2) indicated that SeMSC reduced the growth of PNT1A cells more than DU145 PCa cells by about 10–40%. SeM at the highest concentration caused a slight growth inhibition of PNT1A (69% viability) and DU145 (85% viability). SeMSC decreased cell proliferation of PNT1A and DU145 more than SeM by approximately 30%.

Hoechst nuclear staining was used to monitor the morphological changes that occurred after PNT1A cells and DU145 PCa cells were incubated with SeM or SeMSC (20–300 μM). Untreated normal prostate cells (without exposure to selenium) served as control samples (Figs. 3–6). After 24 hr incubation with SeM or SeMSC, PNT1A cells exhibited greater morphological changes than DU145 PCa cells with increasing

concentrations of SeM and SeMSC. No change was apparent at the lowest concentration of 20 μM of SeM-incubated normal prostate cells. At 100 μM SeM, PNT1A cells (Fig. 7) appeared slightly shrunken into an angular or irregular shape. At the highest concentration of SeM (300 μM), grayscale fluorescence image of stained PNT1A nuclei revealed chromatin condensation, nuclear fragmentation, and margination characteristics of apoptosis and possibly necrosis (Fig. 8) (Sinha & El-Bayoumy 2004; Elmore 2007; Bai & Wang 2014; Walsh 2014). PNT1A cells treated with SeMSC showed a different pattern of cell morphology not characteristic of apoptosis. Neither nuclear fragmentation nor margination was observed but cell rounding or shrinking and formation of few cytoplasmic vacuoles could be discerned (Figs. 9 &10).

Loss of mitochondrial membrane potential, an indicator of cellular apoptosis, was checked using tetramethylrhodamine methyl ester (TMRM), a cell permeant cationic red fluorescent dye (Griffin et al. 2011; Joshi & Bakowska 2011). SeM or SeMSC treatment of PNT1A at 300 μM concentrations produced partial loss of TMRM puncta, indicating collapse of mitochondrial membrane potential (Figs. 12 & 14). In addition, crystal violet staining (Ito 1984; Lane 2001) of the cells indicated loss of cellular membrane and reduced cell growth in PNT1A cells exposed to 300 μM SeMSC (Fig. 13) but not in SeM-incubated cells (Fig. 11). Compared to the control (Fig. 15), fluorescence microscopy images of fixed SeM- (Figs. 16 & 17) and SeMSC-treated (Fig. 18) DU145 PCa cells indicated no significant morphological changes except for a small amount of apoptotic cells caused by SeM (300 μM, Fig. 17), showing that this PCa cell line was less affected by the inhibitory effects of either SeM or SeMSC.

^{1}H NMR spectroscopy of selenium-treated human prostate cells.—Acquired ^{1}H NMR spectra of non-tumorigenic PNT1A prostate cells and DU145 PCa cells are shown in Figs. 19–24. Control NMR data are cell samples without selenium compounds (Figs. 19 & 22). Peaks were calibrated and corrected based on a TMSP standard (0 ppm), and were assigned according to literature values (Govindaraju et al. 2000). Metabolite concentrations for an average of $\sim 10^6$ cells were calculated based on an internal TMSP standard (1.4 mM) and were corrected depending on the number of protons under the peak. Only those specific metabolite protons that were observed distinctly with relatively minimum overlap in the ^{1}H NMR data were chosen for calculations. It should be noted that the NMR spectra collected only represented intact cells at the end of post-treatment period and metabolites released during the incubation period including extracellular SeM and SeMSC were removed by washing or rinsing with PBS in D_2O prior to NMR experiment. Table 1 shows the percent relative change (positive values for increase or negative values for decrease) in peak area of the metabolites after treatment with selenium compounds. More specifically, the four trellis plots in Fig. 25 show percent changes in all metabolites in all three trials were negative for PNT1A cells except glycine—where positive percent change occurred in all three trials for SeM-treated cells. Percent changes in metabolites were both positive and negative for DU145 cells, particularly, lactate in SeMSC-treated cells. SeMSC produced greater percent changes, either negative or positive. The overall pattern of all twelve metabolites in the four plots appears to be different from one another implying that it is possible not only to distinguish normal cells from cancerous cells but also whether SeM or SeMSC was used.

Statistical analysis.—Factor analysis (FA) is a statistical procedure that reduces a large number of factors to a smaller more interpretable number of factors in a dataset. The FA method was applied to the acquired NMR data to determine which changes in the concentration levels of the metabolites would indicate prostate cells were normal or cancerous and the type of treatment performed. Results from the two factor FA analysis in Fig. 26 &27 showed a separation of cancerous cells from normal cells: trials 1, 2 and 3 of DU145 SeM (upper left part of plot) are separate from trials 1, 2 and 3 of PNT1A SeM (lower right part of plot). Oblique components RC1 (standardized loadings 0.87, 0.98, 0.72, 0.36, –0.01, –0.20 for three trials of normal and cancerous cells, respectively) and RC2 (standardized loadings 0.14, –0.09, 0.03, 0.76, 0.76, 0.80 for three trials of normal and cancerous cells, respectively) had 0.41 correlation and communality values $h^2 = 0.88$, 0.89, 0.54, 0.93, 0.57 and 0.54, respectively, described 41% and 31% respectively of the variation in the loadings, a total of 72% of the total variation in all twelve variables. However, trials 1, 2 and 3 of DU145 SeMSC are not

Table 1.—Percent relative change of ^{1}H NMR detectable metabolite levels of SeM- and SeMSC-treated PNT1A non-tumorigenic prostate cells and DU145 PCa cells. Change in metabolite concentrations were measured relative to untreated cell samples (control). Results are average of three independent cell preparations. Abbreviations used: Ala, alanine; Cr, creatine; Cho, choline; PC, phosphocholine; GPC, glycerophosphocholine; Tau, taurine; Gly, glycine; Lac, lactate; β-Glc, β-glucose; UDP, uridine 2′-diphosphate; NADP, nicotine adenine dinucleotide phosphate.

Metabolites	δ ^{1}H ppm	Number of H's	Conc mM per $\sim 10^{6}$ untreated control		PNT1A cells		DU145 PCa cells	
			PNT1A cells	DU145 cells	SeM	SeMSC	SeM	SeMSC
Lipids	1.31	2	0.448 ± 0.057	0.240 ± 0.053	−56.1 ± 12.6	−75.4 ± 3.64	−28.3 ± 7.9	−54.9 ± 1.4
Ala	1.50	3	0.120 ± 0.001	0.098 ± 0.023	−23.3 ± 5.7	−55.8 ± 1.1	−35.8 ± 8.8	−12.3 ± 25.9
Cr	3.05	3	0.135 ± 0.008	0.050 ± 0.010	−56.1 ± 10.4	−80.7 ± 1.2	−25.0 ± 14.4	−35.4 ± 17.1
Cho	3.21	9	0.017 ± 0.003	0.013 ± 0.003	−45.8 ± 16.4	−70.3 ± 6.6	10.0 ± 5.1	−39.7 ± 15.5
PC	3.23	9	0.113 ± 0.007	0.026 ± 0.008	−59.6 ± 2.2	−54.4 ± 3.1	−34.2 ± 7.2	−5.7 ± 7.8
GPC	3.24	9	0.024 ± 0.000	0.011 ± 0.003	−33.3 ± 17.1	−58.3 ± 5.5	5.4 ± 16.5	−35.2 ± 7.7
Tau	3.42	2	0.068 ± 0.010	0.166 ± 0.038	−10.9 ± 1.6	−19.2 ± 5.8	−14.8 ± 9.3	−29.0 ± 8.6
Gly	3.55	2	0.084 ± 0.011	0.061 ± 0.021	25.4 ± 12.9	−57.5 ± 3.8	−4.2 ± 12.3	−17.5 ± 2.5
Lac	4.09	1	0.523 ± 0.015	0.364 ± 0.057	−25.9 ± 7.2	−31.9 ± 3.7	11.4 ± 33.4	65.6 ± 50.4
β-Glc	4.63	1	0.322 ± 0.057	0.431 ± 0.152	−60.8 ± 21.3	−64.0 ± 14.2	−37.7 ± 4.1	−28.9 ± 20.5
UDP	7.98	1	0.084 ± 0.000	0.061 ± 0.027	−33.3 ± 9.6	−61.1 ± 11.1	0 ± 0.0	−35.2 ± 17.7
NADP	8.53	1	0.070 ± 0.000	0.047 ± 0.015	−40.0 ± 0.0	−30.0 ± 5.7	0 ± 0.0	−75.0 ± 25.0

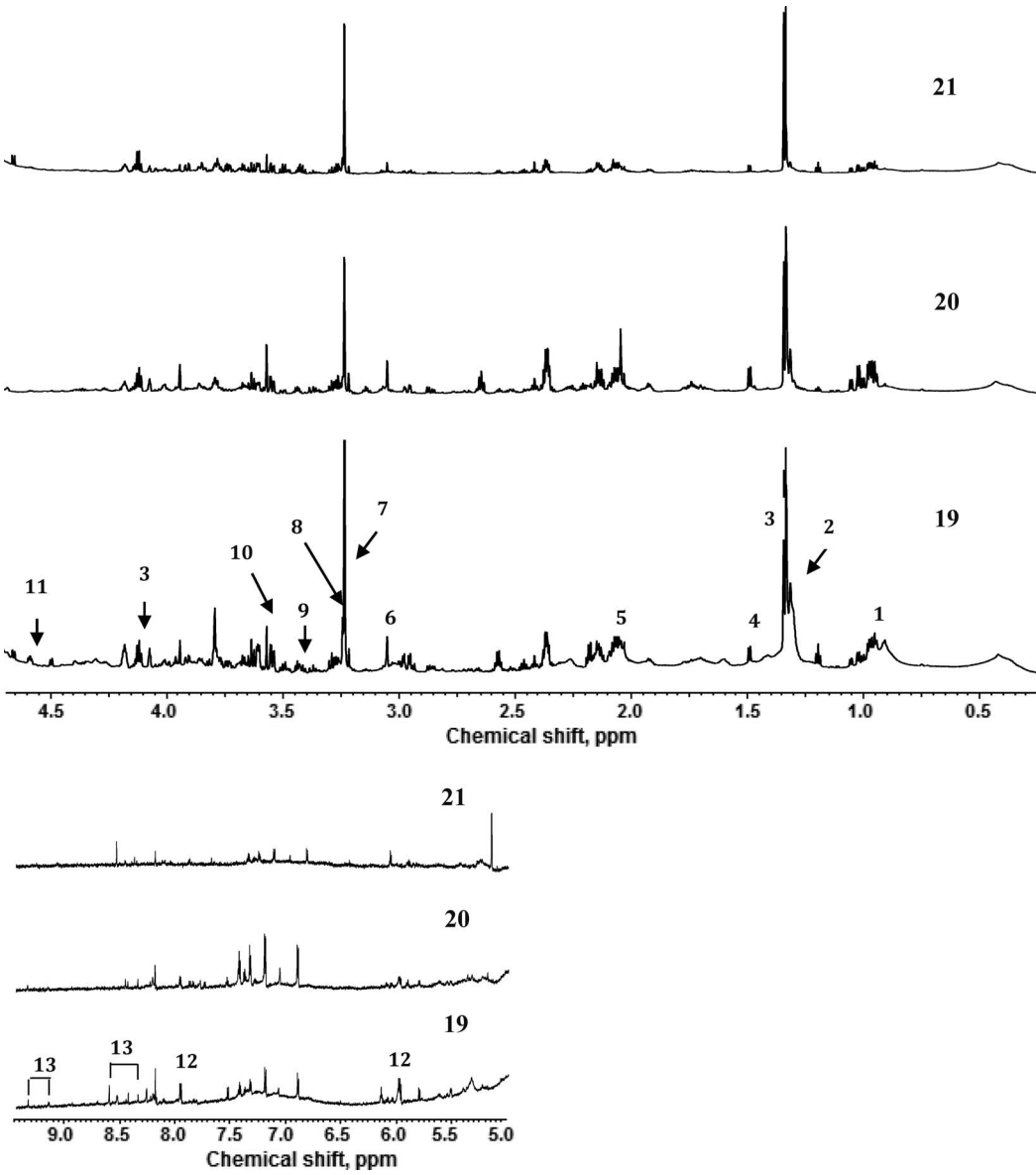

Figures 19–21.—^{1}H NMR spectra (0.25-8.7 ppm) of non-tumorigenic PNT1A prostate cells (19), and after treatment with 300 μM SeM (20) and SeMSC (21). 1: Lipids CH_3, branched chain amino acids; 2: Lipids CH_2; 3: Lactate (Lac); 4: Alanine (Ala); 5: Glutamine (Gln), Glutamic acid (Glu); 6: Creatine (Cr); 7: Choline (Cho), Phosphocholine (PC); 8: Glycerophosphocholine (GPC); 9: Taurine (Tau); 10: Glycine (Gly); 11: β-Glucose (β-Glc); 12: Uridine 5′-diphospho-*N*- acetylglucosamine or Uridine 5′-diphospho-*N*-acetylgalactosamine (UDP); 13: Nicotinamide adenine dinucleotide 2′- diphosphate ($NADP^+$).

grouped separately from trials 1, 2 and 3 of PNT1A SeMSC (Fig. 27). These two factor analyses indicate, in spite of the small sample size of 12 trials and possible dangers of spurious correlations due to the use of percent change data, the measurements of all twelve metabolites reacting to SeM (but not SeMSC) are able to distinguish between normal (PNT1A) and cancerous (DU145) cells, although any one particular metabolite alone was not able to do so. This implies that the lists of metabolite percent reductions given in Table 1

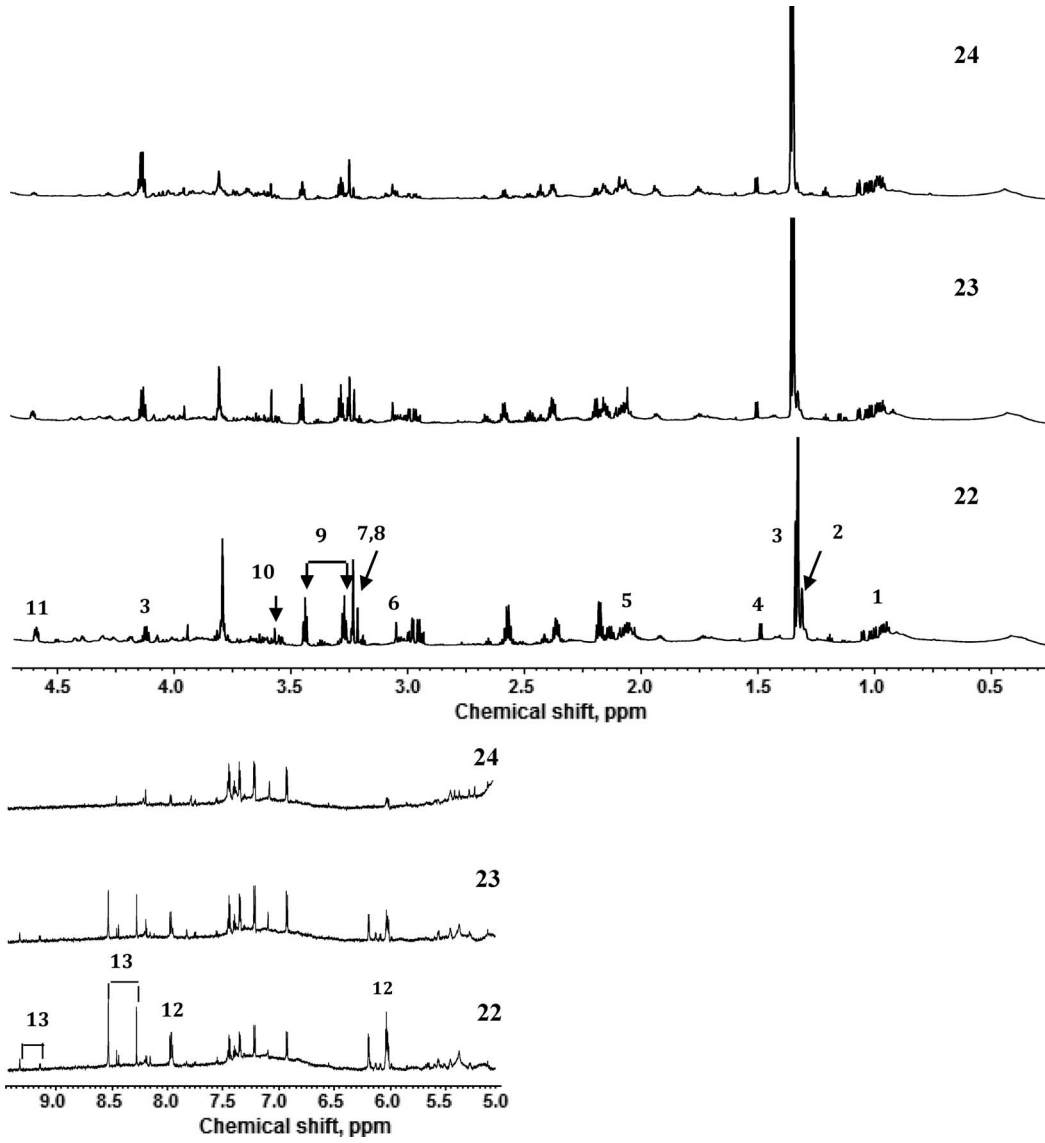

Figures 22–24.—^{1}H NMR spectra (0.25-8.7 ppm) of DU145 prostate cancer cells (22), and after treatment with 300 μM SeM (23) and SeMSC (24). 1: Lipids CH_3, branched chain amino acids; 2: Lipids CH_2; 3: Lactate (Lac); 4: Alanine (Ala); 5: Glutamine (Gln), Glutamic acid (Glu); 6: Creatine (Cr); 7: Choline (Cho), Phosphocholine (PC); 8: Glycerophosphocholine (GPC); 9: Taurine (Tau); 10: Glycine (Gly); 11: β-Glucose (β-Glc); 12: Uridine 5′-diphospho-*N*- acetylglucosamine or Uridine 5′-diphospho-*N*-acetylgalactosamine (UDP); 13: Nicotinamide adenine dinucleotide 2′- diphosphate ($NADP^+$).

(or Fig. 25) could be used as profiles to identify whether cells were cancerous or not: if, for example, the 12 metabolites of cells incubated with SeM had the same percent reduction as given in the second-to-last column of Table 1, this would indicate these cells were characteristic of DU145 PCa cells.

DISCUSSION

Metabolic alterations of prostate cells responding to selenium treatment are not currently available. In this *in vitro* study, we have conducted metabolic profiling of prostate cells after treatment with SeM and SeMSC. The anticarcinogenic properties of SeM and SeMSC are related to the

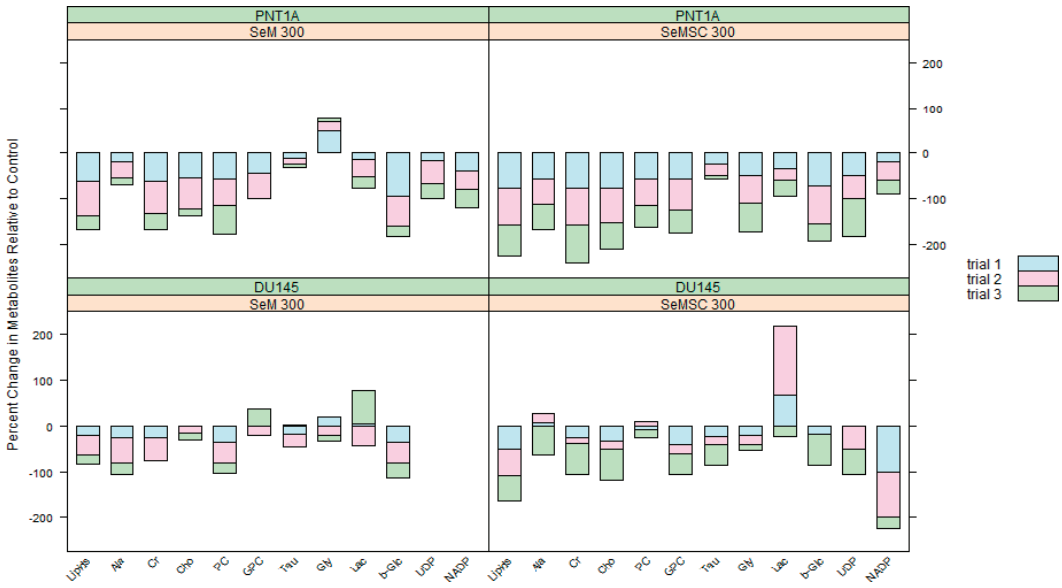

Figure 25.—Bivariate trellis plots of percent changes in three trials of all metabolites relative to control, grouped by PNT1A and DU145 cells and by SeM (300 μM) and SeMSC (300 μM) compounds. Abbreviations used: Ala, alanine; Cr, creatine; Cho, choline; PC, phosphocholine,; GPC, glycerophosphocholine; Tau, taurine; Gly, glycine; Lac, lactate; β-Glc, β-glucose; UDP, uridine 2′-diphosphate; NADP, nicotine adenine dinucleotide phosphate. Note: both UDP and NADP had zero percent changes from control in SeM-treated DU145.

reactive oxygen species (ROS) produced by redox cycling, modification of protein thiols, and induction of DNA strand breaks (Zeng 2009; Sanmartin et al. 2012). Results from NMR data showed perturbations in metabolite levels that correlate with the type of organoselenium and the prostate cells used.

Lactate (2-hydroxypropanoic acid) is the end product of anaerobic glycolysis and is observed to be elevated in metastatic prostate (Moestue et al. 2011), cervical (Walenta et al. 2000), and squamous head and neck (McFate et al. 2008) cancers. Increased glycolysis occurs in tumor cells wherein lactate is produced directly from glucose in the presence of oxygen, known as the Warburg effect (Vander Heiden et al. 2009). The methyl and methine groups of lactate occur as a doublet at 1.31 ppm and a quartet at 4.09 ppm, respectively. After SeM and SeMSC treatment, peak intensity for lactate, based on methine quartet, decreased in PNT1A cells, but increased in DU145 cells (Table 1 and Fig. 25). Results suggest that decreased

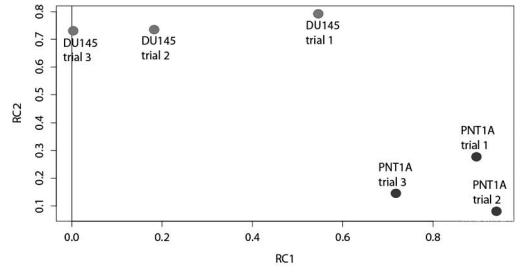

26

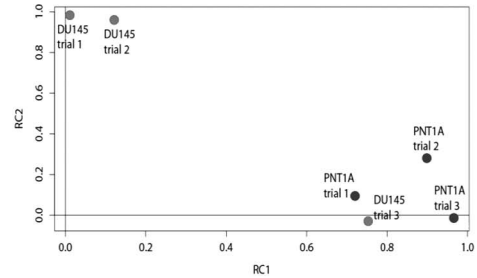

27

Figures 26–27.—Factor analysis diagram of oblimin rotation of two factors based on 6 metabolite percent change data, grouped into (a) PNT1A and DU145 SeM all trials, and (b) PNT1A and DU145 SeMSC all trials.

production of lactate can be attributed to increased lactate metabolism as a result of cell stress and disordered energy metabolism during selenium treatment in PNT1A cells. Increased lactate production in Se-treated DU145 cells reflects the typical hallmark of tumor cell metabolism in which glycolysis is upregulated by converting glucose to lactate in an energy inefficient manner. Lactate is also responsible for the consistently acidic environment of tumor tissues enhancing tumor invasion *in vitro* and increased metastasis *in vivo* (Walenta et al. 2000; McFate et al. 2008).

Alanine contains methyl and methine groups similar to lactate with a doublet at 1.50 ppm and a quartet at 3.77 ppm. In our study, a decrease in alanine concentration was detected in both prostate cell lines after selenium treatment. A decrease in alanine concentration was identified in apoptosis-induced HT-29 cells following an initial increase (Lutz et al. 2003).

Glycine is a catabolic product of choline through the choline biosynthetic pathway via irreversible oxidation to betaine producing sarcosine (*N*-methylglycine) as an intermediate product, which is eventually metabolized to glycine (Locasale 2013). High levels of glycine, as a result of increased choline concentration in cancerous tissues, have been proposed as a biomarker for malignancy, and glycine concentration has been shown to decrease in response to drug therapy (Davies et al. 2008, 2010; Mirbahai et al. 2011). In SeM-treated PNT1A prostate cells in this study, the amount of cellular glycine increased by about 25% (Table 1), but decreased in SeMSC-treated cells by 58%. In contrast, glycine only decreased by approximately 4–18% in DU145 PCa Se-treated cells.

Phosphocholine is a metabolic product from phosphatidylcholine that forms the typical cellular membrane bilayer structure with phosphorylethanolamine and other neutral lipids controlling membrane integrity. Elevated levels of phosphocholine and choline-containing compounds have been established as characteristics of cancers of the breast and prostate, as well as other types of solid tumors (Ackerstaff et al. 2003). High levels of choline and choline-containing metabolites have been postulated to correlate with induced membrane transport and upregulation of phospholipases and choline kinase activity taking place in the Kennedy pathway during carcinogenesis (Oakman et al. 2011; Podo et al. 2011). Choline-containing metabolites in malignant human prostatic epithelial cell line (LNCaP, DU145, TSU and PC-3) have been quantified using ^{1}H NMR spectroscopy and results demonstrated that the amount of choline compounds (or total choline) calculated to be 0.4–4.5 mM per 100–250 cells is significantly higher than non-tumoral epithelial cells determined to be ~0.02–0.2 mM (Ackerstaff et al. 2001). Compared to untreated cells in our study, there is a general reduction in the peak area for choline (3.21 ppm) and phosphocholine (3.23 ppm) for both Se-treated normal and PCa cells (Table 1), demonstrating the significance of phospholipid precursors as biochemical indicators of cells responding to selenium treatment. Decrease in total choline in DU145 SeMSC-treated PCa cells is in agreement with published data in which a marked decrease in choline-containing metabolites was observed in doxorubicin-induced or ionizing radiation-induced apoptotic HL60 leukemia cells (Rainaldi et al. 2008) as well as in *in vivo* rat liver cell apoptosis induced by high dose sodium selenite (Cao et al. 2008).

Creatine is a high-energy metabolite linked with choline metabolism. In our study, SeMSC treatment of PNT1A prostate cells caused a significant decrease in the amount of cellular creatine (81%, Table 1). Creatine/creatine kinase system plays an important role in cellular energy regulation and transport, especially in cells with high and disrupted energy metabolism (Wang et al. 2013; Onda et al. 2006). A reduced amount of creatine has been identified in thymidine kinase-ganciclovir gene therapy treated rat glioma cells (Lehtimäki et al. 2003; Valonen et al. 2005).

Taurine (2-aminomethanesulfonic acid) is an amino acid that functions in maintaining cell osmoregulation (Schaffer et al. 2000). In our study, the quantity of taurine in DU145 cells is approximately three times more than the amount detected in PNT1A cells. Others observed that an elevated taurine concentration is associated with increased malignancy in human cerebral neoplasms (Peeling & Sutherland 1992; Kovanlikaya et al. 2005). Studies conducted on apoptotic rat brain glioma cells and in HL60 leukemia cells showed a substantial decline in taurine signal (Friis et al. 2005; Rainaldi et al. 2008), which coincides with results of the present study. Peak area of taurine resonances for SeM- or SeMSC-treated PNT1A and DU145 cells compared to untreated control (Figs. 19–24) was calculated to decrease by 11–29% (Table 1). In contrast, other investigations reported an increase in taurine

concentration during apoptosis in a variety of cell types such as cerebellar neurons (Moreno-Torres et al. 2004), 3T3 fibroblasts (Friis et al. 2005), and glioblastomas (Opstad et al. 2009; Opstad 2012). The study conducted on 3T3 fibroblasts showed that protein kinase activation results in cysteine protease caspase-3 stimulation before an efflux of potassium and taurine from the cell, enhancing DNA fragmentation and cell shrinkage characteristic of apoptosis (Friis et al. 2005). However, accumulation of taurine was also observed in necrotic HL60 leukemia cells (Rainaldi et al. 2008).

Glucose is an essential source of cellular energy and serves as a precursor for various biochemical compounds. Peak intensity for β-glucose at 4.63 ppm exhibited a decline of approximately 29–64% for both prostate cell lines after selenium treatment (Figs. 19–24). Accurate peak integration of α-glucose at 5.22 ppm is complicated by the proximity of the proton signal with water resonance during water suppression experiment; therefore, result for α-glucose was omitted.

UDPs, which correspond to both uridine 5′-diphospho-*N*-acetylglucosamine (UDP-GlcNAc) and uridine 5′-diphospho-*N*-acetylgalactosamine (UDP-GalNAc), are nucleotide sugar precursor molecules in lipid glycosylation and in polypeptide biosynthetic pathways. Mediated by the hexosamine pathway, glucose is converted to uridine 5′-diphospho-*N*-acetylhexosamine (UDP-GNAc), which is subsequently synthesized to glycoproteins, proteoglycans, and glycolipids (Lau & Dennis 2008). Some glycosylation metabolic pathways are identified to be involved in tumor progression (Grande et al. 2011). The presence of UDP may imply increase synthesis of nucleotides necessary for replication of proliferative cells. Based on uracil (U_6) signal at 7.98 ppm, UDP showed no change or a 33–61% decline in peak intensity upon selenium treatment of prostatic cells relative to untreated cells (Table 1). Previous studies on human glioblastoma cells indicate that cell death does not cause an increase in UDP-GlcNAc or UDP-GalNAc levels (Opstad 2012), while cisplatin-treated rat brain cells showed elevated amounts of UDP-GlcNAc and UDP-GalNAc as a result of reduced activity of UDP-*N*-acetylglucosamine-polypeptide-*N*-acetylglucosaminyl transferase during cell stress (Pan et al. 2011).

Strong lipid signals originating from saturated methyl at 0.9 ppm and methylene at 1.3 ppm are evident as shown in Figs. 19–24. A lipid proton peak at 1.31 ppm, which is resolved from lactate resonance, indicated a significant decrease in intensity ranging from 28–76% for both normal and tumorigenic prostate cells upon incubation with SeM or SeMSC. This result does not agree with other *in vitro* studies reporting lipid accumulation of drug-induced apoptosis and necrosis in human prostate (Milkevitch et al. 2005), cervical (Bezabeh et al. 2001), leukemia (Locasale 2013), Jurkat T-cell lymphoblasts (Al-Saffar et al. 2002), and rat gliomas (Lehtimäki et al. 2003). Another study revealed that saturated lipid peaks are present in damaged tumor cells irrespective of cell death mechanism (Kauppinen 2002).

Citrate levels are usually high in normal prostatic tissue and prostatic fluid at a concentration of about 100 mM, but are reduced in malignant prostate cancer cells (Teahan et al. 2011). Citrate signals as doublets at 2.55–2.65 ppm were neither observed in the NMR spectra of DU145 PCa cells nor in PNT1A cells (Figs. 19–24). This clearly implies that normal prostate function marked by high citrate levels is not retained in PNT1A cells. Therefore, generating normal physiological phenotypes in immortalized cell models poses a challenging task. A similar study conducted on a non-malignant prostate epithelial cell line RWPE-1 also indicated absence of citrate peaks (Teahan et al. 2011).

Nicotine adenine dinucleotide (NAD) or nicotine adenine dinucleotide phosphate (NADP) has a complex coupling pattern, and contributions from ribose resonating upfield from the water signal are small and overlap with other metabolites. Proton resonances for the two ribose moieties at 4.26–6.15 ppm occur in the most crowded region of the spectrum and are not clearly discernible. Aromatic pyridine (at 8.31–9.44 ppm) and adenine-ring (at 8.42–8.52 ppm) protons are pH-dependent and are sometimes not distinctly apparent due to slow exchange with water (Govindaraju et al. 2000). Selenium-treated prostate cells showed no change or a decrease in NADP level by 30–75% based on pyridine proton at 8.53 ppm (Table 1). Relatively small peak intensities associated with NADP protons caused large variations in the calculated values.

In summary, results from NMR data indicated that greater alterations in metabolite levels were induced by SeMSC than by SeM treatment. Fluorescence microscopy images showed more morphological changes for SeMSC-incubated prostate cells than SeM-treated cells. The weaker anticancer effect of SeM observed in this study is

in agreement with previous studies indicating that SeM anticancer activity can be enhanced enzymatically by methioninase which catalyzes the formation of superoxide and other SeM metabolites responsible for its anticancer activity (Zhao et al. 2006). SeMSC does not need to be induced enzymatically for it to cause an anticancer effect. Greater cellular changes were also observed in non-tumorigenic PNT1A than DU145 PCa cells suggesting that PCa cells may have a mechanism of protection triggered by the oxidizing property of selenium compounds, and SeM and SeMSC may be producing an undesirable proliferative effect on PCa cells rather than a destructive effect. Recent studies on dietary antioxidants suggest these compounds initiate biochemical pathways that stimulate cancer cell proliferation and neoplastic transformations (Chandel & Tuveson 2014; Sayin et al. 2014). The NMR data showed a higher taurine content in DU145 PCa cells compared to the non-tumorigenic PNT1A cells due mainly to the origin of the metastasis. DU145 is an androgen-independent and poorly-differentiated human prostate cancer cell line of moderate metastatic potential derived from brain metastasis. Taurine, found to be abundant in the human brain, functions as a neuromodulator, neurotransmitter, and an osmolyte.

Reduced concentrations of metabolites observed with selenium treatment suggested catastrophic collapse of viable cells with the greatest change demonstrated by creatine, a high-energy metabolite. However, lactate, choline-containing compounds (Cho and GPC), and glycine levels increased depending on the type of selenium used and the cell type. No clear pattern of variation in metabolite concentration levels to distinguish apoptotic versus non-apoptotic pathway was observed probably due to heterogeneity of the harvested cells utilized during NMR acquisition, and the possibility that more than one cell death pathway (Chaabane et al. 2013; Su et al. 2013) was induced simultaneously by SeM and SeMSC.

Statistical analysis by FA method performed in this study, based on the change in the concentration levels of twelve metabolites determined by ^{1}H NMR spectroscopy, was able to distinguish between normal (PNT1A) and cancerous (DU145) cells for SeM-treated cells, although any one particular metabolite alone was not able to do so as shown in Figs. 26 &27.

NMR spectroscopy is a valuable tool in monitoring cellular response upon drug treatment. In this study, ^{1}H NMR was exploited to assess the effect of organoselenium treatment of non-tumorigenic and tumorigenic prostate cell lines. Although the exact cell death mechanism stimulated by the selenium compounds used was not established spectrometrically, NMR spectral data confirmed microscopy results that SeMSC triggered more cell stress response in the prostate cell lines used. The results in this study represent one of the first sets of NMR spectroscopic data in metabolic profiling of selenium-treated prostate cells coupled with pattern recognition techniques. Obtaining more complete information of biochemical processes occurring during treatment is an important step towards a better understanding of cellular processes that can have future applications in the clinical setting to monitor treatment response and to improve management of anticancer therapy.

ACKNOWLEDGMENTS

This research was financially supported by the Indiana Academy of Science Senior Grant 2012. The authors wish to thank Purdue University North Central Biology/Chemistry Department for resources, Betsy Papka (Chemistry Stockroom Manager), Prof. Kevin Jantzi (Valparaiso University) for the use of 400 MHz NMR spectrometer, Prof. Marc Anderson (San Francisco State University Chemistry Department) for the use of ACDLabs NMR Processing software, and Wee Tam (San Francisco State University Chemistry Department) for initial NMR assistance.

CONFLICT OF INTEREST

Authors declare that they have no conflict of interest.

COMPLIANCE WITH ETHICAL REQUIREMENTS

This article does not contain any studies with human or animal subjects.

LITERATURE CITED

Abdulah, R., K. Kobayashi, C. Yamazaki & H. Koyama. 2011. Molecular targets of selenium in prostate cancer prevention (Review). International Journal of Oncology 39:301–309.

Ackerstaff, E., K. Glunde & Z.M. Bhujwalla. 2003. Choline phospholipid metabolism: a target in cancer cells. Journal of Cellular Biochemistry 90:525–533.

Ackerstaff, E., B.R. Pflug, J.B. Nelson & Z.M. Bhujwalla. 2001. Detection of increased choline

compounds with ^{1}H NMR spectroscopy following malignant transformation of human prostatic epithelial cells. Cancer Research 61:3599–3603.

Al-Saffar, N.S., J.C. Titley, D. Robertson, P.A. Clarke, L.E. Jackson, M.O. Leach & S.M. Ronen. 2002. Apoptosis is associated with triacylglycerol accumulation in Jurkat T-cells. British Journal of Cancer 86:963–970.

Bai, L. & S. Wang. 2014. Targeting apoptosis pathways for new cancer therapeutics. Annual Reviews of Medicine 65:139–155. [Doi: 10.1146/annurev-med-010713-141310].

Beger, R.D. 2013. A review of applications of metabolomics in cancer. Metabolites 3:552–574.

Bezabeh, T., M.R.A. Mowat, L. Jarolim, A.H. Greenberg & I.C.P. Smith. 2001. Detection of drug-induced apoptosis and necrosis in human cervical cells using ^{1}H NMR spectroscopy. Cell Death and Differentiation 8:219–224.

Cao, Z., L-P. Wu, Y-X. Li, Y-B. Guo, Y-W. Chen & R-H. Wu. 2008. Change of choline compounds in sodium selenite-induced apoptosis of rats used as quantitative analysis by *in vitro* 9.4T MR spectroscopy. World Journal of Gastroenterology 14:3891–3896.

Chaabane, W., S.D. User, M. El-Gazzah, R. Jaksik, E. Sajjadi, J. Rzeszowska-Wolny & M.J. Los. 2013. Autophagy, apoptosis, mitoptosis and necrosis: interdependence between those pathways and effects on cancer. Archivum Immunologiae et Therapia Experimentalis 61:43–58.

Chandel, N.S. & D.A. Tuveson. 2014. The promise and perils of antioxidants for cancer patients. New England Journal of Medicine 371:177–178.

Chen, Y-C., K.S. Prablu & A.M. Mastro. 2013. Is selenium a potential treatment for cancer metastasis? Nutrients 5:1149–1168. [Doi: 10.3390/nu5041149].

Cornel, E.B., G.A.H.J. Smits, J.E. de Ruijter, G.O.N. Oosterjof, A. Heerschap, F.M.J. Debruyne & J.A. Schalken. 1995. *In vitro* proton magnetic resonance spectroscopy of four human prostate cancer cell lines. The Prostate 26:275–280.

Davies, N.P., M. Wilson, L.M. Harris, K. Natarajan, S. Lateef & L. MacPherson. 2008. Identification and characterization of childhood cerebellar tumors by *in vivo* proton MRS. NMR in Biomedicine 21:908–918.

Davies, N.P., M. Wilson, K. Natarajan, Y. Sun, L. MacePherson & M-A. Brundler. 2010. Non-invasive detection of glycine as a biomarker of malignancy in childhood brain tumors using in-vivo ^{1}H MRS at 1.5 Tesla confirmed by *ex-vivo* high-resolution magic angle spinning NMR. NMR in Biomedicine 23:80–87.

DeFeo, E.M. & L.L. Cheng. 2010. Characterizing human cancer metabolomics with *ex vivo* HRMAS MRS. Technology in Cancer Research and Treatment 9:381–391.

DeFeo, E.M., C-L. Wu, W.S. McDougal & L.L. Cheng. 2011. A decade in prostate cancer: from NMR to metabolomics. Nature Reviews Urology 8:301–311.

Dunn, B.K., E.S. Richmond, L.M. Miansian, A.M. Ryan & L.G. Ford. 2010. A nutrient approach to prostate cancer prevention: the selenium and vitamin E cancer prevention trial (SELECT). Nutrition and Cancer 62:896–918.

Elmore, S. 2007. Apoptosis: a review of programmed cell death. Toxicologic Pathology 35:495–516.

Friis, M.B., C.R. Friborg, L. Schneider, M.B. Nielsen, I.H. Lambert, S.T. Christensen & E.K. Hoffmann. 2005. Cell shrinkage as a signal to apoptosis in NIH 3T3 fibroblasts. Journal of Physiology 567:427–443.

Giskeødegård, G.F., H. Bertilsson, K.M. Selnæs, A.J. Wright, T.F. Bathen, T. Viset, J. Halgunset, A. Angelsen, I.S. Gribbestad & M-B. Tessem. 2013. Spermine and citrate as metabolic biomarkers for assessing prostate cancer aggressiveness. PLoS ONE, 8, e62375.doi:10.1371/journal.pone.0062375.

Goulet, A-C., M. Chigbrow, P. Frisk & M.A. Nelson. 2005. Selenomethionine induces sustained ERK phosphorylation leading to cell-cycle arrest in human colon cancer cells. Carcinogenesis 26:109–117.

Govindaraju, V., K. Young & A.A. Maudsley. 2000. Proton NMR chemical shifts and coupling constants for brain metabolites. NMR in Biomedicine 13:129–153.

Grande, S., A. Palma, A.M. Luciani, A. Rosi, L. Guidoni & V. Viti. 2011. Glycosidic intermediates identified in ^{1}H MR spectra of intact tumour cells may contribute to the clarification of aspects of glycosylation pathways. NMR in Biomedicine 24:68–79.

Griffin, C., J. McNulty & S. Pandey. 2011. Pancreastatin induces apoptosis and autophagy in metastatic prostate cancer cells. International Journal of Oncology 38:1549–1556.

Hurst, R., L. Hooper, T. Norat, R. Lau, D. Aune, D.C. Greenwood, R. Vieira, R. Collings, L.J. Harvey, J.A.C. Sterne, R. Beynon, J. Savović & S.J. Fairweather-Tait. 2012. Selenium and prostate cancer: systematic review and meta-analysis. American Journal of Clinical Nutrition 96:111–122.

Ito, M. 1984. Microassay for studying anticellular effects of human interferons. Journal of Interferon Research 4:603–608.

Jackson, M.I. & G.F. Combs Jr. 2008. Selenium and anticarcinogenesis: underlying mechanisms. Current Opinion in Clinical Nutrition and Metabolic Care 11:718–726. [Doi: 10.1097/MCO.0b013e3283139674].

Jordan, K.W. & L.L. Cheng. 2007. NMR-based metabolomics approach to target biomarkers for human prostate cancer. Expert Review of Proteomics 4:389–400.

Joshi, D.C. & J.C. Bakowska. 2011. Determination of mitochondrial membrane potential and reactive oxygen species in live rat cortical neurons. Journal of Visualized Experiments 51:2704:1–4.

Kabacoff, R.I. R in Action: Data Analysis and Graphics with R. 2011. Manning Publications Co., Shelter Island, New York. 608 pp.

Kauppinen, R.A. 2002. Monitoring cytotoxic tumour treatment response by diffusion magnetic resonance imaging and proton spectroscopy. NMR in Biomedicine 15:6–17.

Kim, T., U. Jung, D-Y. Cho & A-S. Chung. 2001. Se-methylselenocysteine induces apoptosis through caspase activation in HL-60 cells. Carcinogenesis 22:559–565.

Kovanlikaya, A., A. Panigrahy, M.D. Krieger, I. Gonzalez-Gomez, N. Ghugre, J.G. Mccomb, F.H. Gilles, M.D. Nelson & S. Blümi. 2005. Untreated pediatric primitive neuroectodermal tumor *in vivo*: quantitation of taurine with MR Spectroscopy. Radiology 236:1020–1025.

Kristal, A.R., A.K. Darke, J.S. Morris, C.M. Tangen, P.J. Goodman, I.M. Thompson, F.L. Mevskens Jr., G.E. Goodman, L.M. Minasian, H.L. Parnes, S.M. Lippman, & E.A. Klein. 2014. Baseline selenium status and effects of selenium and vitamin E supplementation on prostate cancer risk. Journal of National Cancer Institute 106:1–8. [Doi: 10.1093/jnci/djt456].

Lane, T. 2001. Crystal violet (CV) staining of cells and clone counting, Mcbd.ucla.edu. At: https://www.mcdb.ucla.edu/Research/ Arispe/Protocols/CV_Staining_of_Cells.pdf (Accessed 4 April 2014).

Lau, K.S. & J.W. Dennis. 2008. N-Glycans in cancer progression. Glycobiology 18:750–760.

Ledesma, M.C., B. Jung-Hynes, T.L. Schmit, R. Kumar, H. Mukhtar & N. Ahmad. 2011. Selenium and vitamin E for prostate cancer: post-SELECT (Selenium and Vitamin E Cancer Prevention Trial) status. Molecular Medicine 17:134–143.

Lee, S.O., J.Y. Chun, N. Nadiminty, D.L. Trump, C. Ip, Y. Dong & A.C. Gao. 2006. Monomethylated selenium inhibits growth of LNCaP human prostate cancer xenograft accompanied by a decrease in the expression of androgen receptor and prostate-specific antigen (PSA). The Prostate 66:1070–1075.

Lehtimäki, K.K., P.K. Valonen, J.L. Griffin, T.H. Väisänen, O.H. Gröhn, M.I. Kettunen, J. Vepsalainen, S. Ylä-Herituala, J. Nicholson & R.A. Kauppinen. 2003. Metabolite changes in BT4C rat gliomas undergoing ganciclovir-thymidine kinase gene therapy-induced programmed cell death as studied by ^{1}H NMR spectroscopy *in vivo*, *ex vivo*, and *in vitro*. Journal of Biological Chemistry 278:45915–45923.

Levin, Y.C., M.J. Albers, T.N. Butler, D. Spielman, D.M. Peehl & J. Kurhanewicz. 2009. Methods of metabolic evaluation of prostate cancer cells using proton and ^{13}C HR-MAS spectroscopy and [3-^{13}C] pyruvate as a metabolic substrate. Magnetic Resonance in Medicine 62:1091–1098.

Li, G.X., H.J. Lee, Z. Wang, H. Hu, J.D. Liao, J.C. Watts, G.F. Combs Jr. & J. Lü. 2008. Superior *in vivo* inhibitory efficacy of methylseleninic acid against human prostate cancer over selenomethionine or selenite. Carcinogenesis 29:1005–1012.

Lin, G. & Y-L. Chung. 2014. Current opportunities and challenges of magnetic spectroscopy, positron emission tomography, and mass spectrometry imaging for mapping cancer metabolism *in vivo*. BioMedical Research International 625095:1–13.

Locasale, J.W. 2013. Serine, glycine and one-carbon units: cancer metabolism in full circle. Nature Reviews Cancer 13:572–583.

Lutz, N.W., M.E. Tome & P.J. Cozzone. 2003. Early changes in glucose and phospholipid metabolism following apoptosis induction by IFN-gamma/TNF-alpha in HT-29 cells. FEBS Letters 544:123–128.

MacKinnon, N., A.P. Khan, A.M. Chinnaiyan, T.M. Rajendiran & A. Ramamoorthy. 2012. Androgen receptor activation results in metabolite signatures of an aggressive prostate cancer phenotype: an NMR–based metabonomics study. Metabolomics 8:1026–1036.

McFate, T., A. Mohyeldin, H. Lu, J. Thakar, J. Henriques, M.D. Halim, H. Wu, M.J. Schell, T.M. Tsang, O. Teahan, S. Zhou, J.A. Califano, N.H. Jeoung, R.A. Harris & A. Verma. 2008. Pyruvate dehydrogenase complex activity controls metabolic and malignant phenotype in cancer cells. Journal of Biological Chemistry 283:22700–22708.

Menter, D.G., A.L. Sabichi & S.M. Lippman. 2000. Selenium effects on prostate cell growth. Cancer Epidemiology, Biomarkers & Prevention 9:1171–1182.

Meuillet, E., S. Stratton, D.P. Cherukuri, A-C. Goulet, J. Kagey, B. Porterfield & M.A. Nelson. 2004. Chemoprevention of prostate cancer with selenium: an update on current clinical trials and preclinical findings. Journal of Cellular Biochemistry 91:443–458.

Milkevitch, M, H. Shim, U. Pilatus, S. Pickup, J.P. Wehrle, D. Samid, H. Poptani, J.D. Glickson & E.J. Delikatny. 2005. Increases in NMR-visible lipid and glycerophosphocholine during phenylbutyrate-induced apoptosis in human prostate cancer cells. Biochimica Biophysica Acta 1734:1–12.

Mirbahai, L., M. Wilson, C.S. Shaw, C. McConville, D.G. Malcomson, J.L. Griffin, R.A. Kauppinen & A.C. Peet. 2011. ^{1}H magnetic resonance spectroscopy metabolites as biomarkers for cell cycle arrest and cell death in rat glioma cells. International Journal of Biochemistry and Cell Biology 43:990–1001.

Moestue, S., B. Sitter, T.F. Bathen, M-B. Tessem & I.S. Griggestad. 2011. HR MAS MR spectroscopy in metabolic characterization of cancer. Current Topics in Medicinal Chemistry 11:2–26.

Moreno-Torres, A., I. Martinez-Pérez, M. Baquero, J. Campistol, A. Capdevila, C. Arús & J. Pujol. 2004. Taurine detection by proton magnetic resonance spectroscopy in medulloblastoma: contribution to noninvasive differential diagnosis with cerebellar astrocytoma. Neurosurgery 55:824–829.

Nelson, M.A., A-C. Goulet, E.T. Jacobs & P. Lance. 2005. Studies into the anticancer effect of selenomethionine against human colon cancer. Annals of New York Academy of Sciences 1059:26–32.

NIH. 2015. Selenium: Dietary Supplement Fact Sheet. At: https://ods.od.nih.gov/factsheets/Selenium-HealthProfessional/

Oakman, C., L. Tenori, L. Biganzoli, L. Santarpia, S. Cappadona, C. Luchinat & A. Di Leo. 2011. Uncovering the metabolic fingerprint of breast cancer. International Journal of Biochemistry and Cell Biology 43:1010–1020.

Onda, T., K. Uzawa, Y. Endo, H. Bukawa, H. Yokoe, T. Shibahara & H. Tanzawa. 2006. Ubiquitous mitochondrial creatine kinase down regulated in oral squamous cell carcinoma. British Journal of Cancer 94:698–709.

Opstad, K.D. 2012. Role of taurine in apoptosis using magnetic resonance spectroscopy. Pp.121–128. *In* Tumors of the Central Nervous System. (M.A. Hayat, Ed.). Springer Publishing Company, New York, New York.

Opstad, K.S., B.A. Bell, J.R. Griffiths & F.A. Howe. 2009. Taurine: a potential marker of apoptosis in gliomas. British Journal of Cancer 100:789–794.

Palmnas, M.S.A. & H.J. Vogel. 2013. The future of NMR metabolomics in cancer therapy: towards personalizing treatment and developing targeted drugs? Metabolites 3:373–396.

Pan, X., M. Wilson, L. Mirbahai, C. McConville, T.N. Arvantis, J.L. Griffin, R.A. Kauppinen & A.C. Peet. 2011. *In vitro* metabonomic study detects increases in UDP-GlcNAc and UDP-GalNAc, as early phase markers of cisplatin treatment response in brain tumor cells. Journal of Proteome Research 10:3493–3500.

Peeling, J. & G. Sutherland. 1992. High-resolution ^{1}H NMR spectroscopy studies of extracts of human cerebral neoplasms. Magnetic Resonance in Medicine 24:123–136.

Pinto, J.T., R. Sinha, K. Papp, N.D. Facompre, D. Desai & K. El-Bayoumy. 2007. Differential effects of naturally occurring and synthetic organoselenium compounds on biomarkers in androgen responsive and androgen independent human prostate carcinoma cells. International Journal of Cancer 120:1410–1417.

Podo, F., S. Canevari, R. Canese, M.E. Pisanu, A. Ricci & E. Iorio. 2011. Tumour phospholipid metabolism. Proceedings of the International Society of Magnetic Resonance in Medicine 19:1–10.

Rainaldi, G., R. Romano, P. Indovina, A. Ferrante, A. Motta, P.L. Indovina & M.T. Santini. 2008. Metabolomics using ^{1}H-NMR of apoptosis and necrosis in HL60 leukemia cells: differences between the two types of cell death and independence from the stimulus of apoptosis used. Radiation Research 169:170–180.

Rayman, M.P. 2005. Selenium in cancer prevention: a review of the evidence and mechanism of action. Proceedings of Nutrition Science 64:527–542.

Reagan-Shaw, S., M. Nihal, H. Ahsan, H. Mukhtar & N. Ahmad. 2008. Combination of vitamin E and selenium causes an induction of apoptosis of human prostate cancer cells by enhancing Bax/Bcl-2 ratio. The Prostate 68:1624–1634.

Reid, M.E., M.S. Stratton, A.J. Lillico, M. Fakih, R. Natarajan, L.C. Clark & J.R. Marshall. 2004. A report of high-dose selenium supplementation: response and toxicities. Journal of Trace Elements in Medicine and Biology 18:69–74.

Richie, J.P. Jr., A. Das, A.M. Calcagnotto, R. Sinha, W. Neidig, J. Liao, E.J. Lengerich, A. Berg, T.J. Hartman, A. Ciccarella, A. Baker, M.G. Kaag, S. Goodin, R.S. DiPaola & K. El-Bayoumy. 2014. Comparative effects of two different forms of selenium on oxidative stress biomarkers in healthy men: a randomized clinical trial. Cancer Prevention Research 7:796–804.

Roberts, M.J., H. Schirra, M. Lavin & R.A. Gardiner. 2014. NMR-based metabolomics: global analysis of metabolites to address problems in prostate cancer. Pp. 1–43. *In* Breast, Cervical and Prostate Cancer. (iConcept Press, Ed.), Tokwawan, Kowloon, Hong Kong.

Sanmartin, C., D. Plano, A.K. Sharma & J.A. Palop. 2012. Selenium compounds, apoptosis and other types of cell death: an overview for cancer therapy. International Journal of Molecular Science 13:9649–9672.

Sayin, V.I., M.X. Ibrahim, E. Larsson, J.A. Nilsson, P. Lindahl & M.O. Bergo. 2014. Antioxidants accelerate lung cancer progression in mice. Science Translational Medicine 6:221 (p221ra15).

Schaffer, S., K. Takahashi & J. Azuma. 2000. Role of osmoregulation in the actions of taurine. Amino Acids 19:527–546.

Seo, Y. R., M.R. Kelley & M.L. Smith. 2002. Selenomethionine regulation of p53 by a ref1-dependent redox mechanism. Proceedings of the National Academy of Science 99:14548–14553.

Serkova, N.J., E.J. Gamito, R.H. Jones, C. O'Donnell, J.L. Brown, S.J. Green, H. Sullivan, T. Hedlund & E.D. Crawford. 2008. The metabolites citrate, myo-inositol, and spermine are potential age-independent markers of prostate cancer in human expressed prostatic secretions. The Prostate 68:620–628.

Shao, W., J. Gu, C. Huang, D. Liu, H. Huang, Z. Huang, Z. Lin, W. Yang, K. Liu, D. Lin & T. Ji. 2014. Malignancy-associated metabolic profiling of human glioma cell lines using ^{1}H NMR spectroscopy. Molecular Cancer 13:1–12. [Doi: 10.1186/1476-4598-13-197].

Siegel, R., K.D. Miller & A. Jemal. 2015. Cancer statistics, 2015. CA: A Cancer Journal for Clinicians 65:5–29.

Singh, C.K., M.A. Ndiaye, I.A. Siddiqui, M. Nihal, T. Havighurst, K-M. Kim, W. Zhong, H. Mukhtar & N. Almad. 2014. Methaneseleninic acid and g-tocopherol combination inhibits prostate tumor growth *in vivo* in a xenograft mouse model. Oncotarget 5:3651–3661.

Sinha, R. & K. El-Bayoumy. 2004. Apoptosis is a critical cellular event in cancer chemoprevention and chemotherapy by selenium compounds. Current Cancer Drug Targets 4:13–28.

Stenman, K., P. Stattin, H. Stenlund, K. Riklund, G. Gröbner & A. Bergh. 2011. ^{1}H HRMAS NMR derived biomarkers related to tumor grade, tumor cell fraction, and cell proliferation in prostate tissue samples. Biomarker Insights 6:39–47.

Stenman, K., I. Surowiec, H. Antti, K. Riklund, P. Stattin, A. Bergh & G. Gröbner. 2010. Detection of local prostate metabolites by HRMAS NMR spectroscopy: a comparative study of human and rat prostate tissues. Magnetic Resonance Insights 4:27–41.

Su, M., Y. Mei & S. Sinha. 2013. Role of the crosstalk between autophagy and apoptosis in cancer. Journal of Oncology 2013:102735. [Doi: 10.1155/2013/102735].

Teahan, O., C.L. Bevan, J. Waxman & H.C. Keun. 2011. Metabolic signatures of malignant progression in prostate epithelial cells. International Journal of Biochemistry and Cell Biology 43:1002–1009.

Thomas, M.A., R. Nagarajan, A. Huda, D. Margolis, M.K. Sarma, K. Sheng, R.E. Reiter & S.S. Raman 2013. Multidimensional MR spectroscopic imaging of prostate cancer *in vivo*. NMR in Biomedicine 27:53–66.

Valonen, P.K., J.L. Griffin, K.K. Lehtimäki, K.K. Nicholson, O.H. Grohn & R.A. Kauppinen. 2005. High-resolution magic-angle spinning ^{1}H NMR spectroscopy reveals different responses in choline-containing metabolites upon gene therapy-induced programmed cell death in rat brain gliomas. NMR in Biomedicine 18:252–259.

Vander Heiden, M.G., C.B. Thompson & L.C. Cantley. 2009. Understanding the Warburg effect: the metabolic requirements of cell proliferation. Science 324:1029–1033.

Vermeersch, K.A. & M.P. Styczynski. 2013. Applications of metabolomics in cancer research. Journal of Carcinogenesis 12:1-9. [Doi: 10.4103/1477-3163.113622].

Vinceti, M., G. Dennert, C.M. Crespi, M. Zwahlen, M. Brinkman, M.P.A. Zeegers, M. Horneber, R. D'Amico & C. Del Giovane. 2015. Selenium for preventing cancer. Cochrane Database Systematic Review 3:CD005195, 1-147. [Doi: 10.1002/14651858.CD005195.pub3].

Walenta, S., M. Wetterling, M. Lehrke, G. Schwickert, K. Sundfor, E.K. Rofstad & W. Mueller-Klieser. 2000. High lactate levels predict likelihood of metastases, tumor recurrence, and restricted patient survival in human cervical cancers. Cancer Research 60:916–921.

Walsh, C.M. 2014. Grand challenges in cell death and survival: apoptosis vs necroptosis. Frontiers in Cell and Developmental Biology 2:3. [Doi: 10.3389/fcell.2014.00003].

Wang, H., L. Wang, H. Zhang, P. Deng, J. Chen, B. Zhou, J. Hu, J. Zou, W. Lu, P. Xiang, T. Wu, X. Shao, Y. Li, Z. Zhou & Y-L. Zhao. 2013. ^{1}H NMR-based metabolic profiling of human rectal cancer tissue. Molecular Cancer 12:121. [DOI: 10.1186/1476-4598-12-121].

Wang, Z., C. Jiang & J. Lü. 2002. Induction of caspase-mediated apoptosis and cell-cycle G_1 arrest by selenium metabolite methylselenol. Molecular Carcinogenesis 34:113–120.

Whitehead, T.L. & T. Kieber-Emmons. 2005. Applying *in vitro* NMR spectroscopy and ^{1}H NMR metabonomics to breast cancer characterization and detection. Progress in Nuclear Magnetic Resonance Spectroscopy 47:165–174.

Yamamoto, N., A. Gupta, M. Xu, K. Miki, Y. Tsujimoto, H. Tsuchiya, K. Tomita, A.R. Moossa & R.M. Hoffman. 2003. Methioninase gene therapy with selenomethionine induces apoptosis in bcl-2-overexpressing lung cancer cells. Cancer Gene Therapy 10:445–450.

Yeo, J-K., S-D. Cha, C-H. Cho, S-P. Kim, J-W. Cho, W-K. Baek, M-H. Shuh, T.K. Kwon, J-W. Park & S-I. Suh. 2002. Se-methylselenocysteine induces apoptosis through caspase activation and Bax cleavage mediated by calpain in SKOV-3 ovarian cancer cells. Cancer Letters 182:83–92.

Zakian, K.L., A. Shukla-Dave, E. Ackerstaff, H. Hricak & J.A. Koutcher. 2008. ^{1}H magnetic resonance spectroscopy of prostate cancer: biomarkers for tumor characterization. Cancer Biomarkers 4:263–276.

Zeng, H. 2009. Selenium as an essential micronutrient: roles in cell cycle and apoptosis. Molecules 14:1263–1278.

Zhao, R., F.E. Domann & W. Zhong. 2006. Apoptosis induced by selenomethionine and methioninase is superoxide mediated and p53 dependent in human prostate cancer cells. Molecular Cancer Therapeutics 5:3275–3284.

Zhong, W. & T.D. Oberley. 2002. Redox-mediated effects of selenium on apoptosis and cell cycle arrest in the LNCaP prostate cancer cell line. Cancer Research 61:7071–7078.

Manuscript received 26 November 2015, revised 22 April 2016.